Gas Processing Journal

Vol. 9, No. 2 2021, pp. 43-52
http://gpj.ui.ac.ir

Research Paper

Influence of specific heat capacity ratio on the optimum design of the leading edge of centrifugal compressor impeller considering the presence of IGV

Jafar Nejadali *
Department of Mechanical Engineering, Faculty of Engineering and Technology, University of Mazandaran, Mazandaran, Iran

Received: 2021-11-29 Revised: 2022-03-14 Accepted: 2022-04-09

Abstract: In this paper, a theoretical analysis was carried out for optimum designing of the leading edge of centrifugal compressor blades. The effect of change in specific heat capacity ratio on the optimal design of impeller blades' leading edge was investigated theoretically considering the inlet pre-whirl. It was found that with the growth in heat capacity ratio, the maximum achievable mass flow function was reduced, while the optimum blade angle at the leading edge was increased. Results showed that the maximum achievable mass flow function for $\gamma = 1.13$, was about 0.77 and occurred at a pre-whirl angle (α) of 60.3° and blade angle (β) of 48.2°. For $\gamma = 1.4$, the maximum achievable mass flow function was about 0.64 and occurred at α=59°, β=51°. For the case of $\gamma = 1.67$, the maximum mass flow function was obtained at about 0.55 and took place at α=57.9°, β=52.7°. It was found that there is a limitation for the hub to shroud radius ratio in impeller designing. The interval between hub to shroud radius is reduced by increasing the angle of inlet guide vanes.
keywords: Centrifugal compressor; Heat capacity ratio; Optimum inlet; Inlet guide vanes; Mach number.

1. Introduction

Centrifugal compressors; also known as turbo-compressors belong to the dynamic type of compressors, meaning that compression is accomplished through the conversion of kinetic energy to static energy. Compared to the axial compressor, the centrifugal compressor has some advantages, such as a single-stage high-pressure ratio, compact structure, and lightweight. Unlike reciprocating compressors, centrifugal compressors are steady-flow devices hence they are subjected to less vibration and noise. These kinds of turbomachines are widespread in applications that require a low mass flow of high-pressure gas [1]. They are used for a variety of technical applications: In metallurgy, chemical and petrochemical engineering, in the gas and pipeline industry, gas turbine engines, automotive turbochargers, and power plants [2].

Achieving high efficiency and wide operating range in centrifugal compressors requires a considerable design effort. The complexity of the flow, especially at the inlet of the centrifugal compressor impeller imposes a challenge on the designer to reach good performance.

Flow non-uniformity at the impeller inlet, which is generally known as “inlet distortion”, has been investigated with experiments and numerical simulations [3, 4]. A zero-dimensional model was proposed by song et al. for the mass flow rate of a compressor with a distorted inlet flow field and the results were compared with 3D CFD data and experiments [5]. To improve stability and stall margin, Yong et al. conducted a numerical analysis for a compressor with ring groove casing treatment. The investigations were done according to the ring groove location. They found that the ring groove increased the operating range [6]. The effect of entry conditions into the impeller (through the change in attack angle along with the blade height) on the performance of the centrifugal compressor was studied numerically by Vanyashov et al. [7]. Yang et al. carried out CFD simulations and experiments to investigate the effects and the

* **Corresponding Author.**
Authors’ Email Address: J. Nejadali (j.nejad@umz.ac.ir

http://10.22108/GPJ.2022.131687.1110

mechanism of stability enhancement by the self-recirculating casing treatment in a centrifugal compressor with a vaneless diffuser [8]. Torregrosa et al. described an experimental study to characterize the behavior of the inlet flow instability of a turbocharger compressor when marginal surge conditions are reached [9]. Galindo et al. performed 3D-CFD simulations to study the impact of placing different geometries, namely a tapered duct, a convergent-divergent nozzle, and a divergent nozzle in the compressor inlet on stability, efficiency, and noise emission [10]. They also presented a specific inlet swirl-generator device (SGD) that extends the surge margin of the compressor [11]. Kim et al. carried out experimental tests to investigate the contribution of three different diffusers to the compressor stage performance, as well as the influence of inlet distortion on performance [12]. To study the influence of the matching between the inlet and outlet distortion on compressor performance, Zheng et al. added two different square wave distortions to the inlet and outlet of a compressor. They found that the matching does have a large influence on the compressor performance and flow field and there does exist the best matching [13]. Recirculation is a flow feature that has a significant impact on compressor performance. Harley et al. studied the inlet recirculation region numerically using several modern automotive turbocharger centrifugal compressors. The point at which the recirculating flow begins to develop and the rate at which it grows were investigated and all numerical data has been validated with experiments [14]. Zamiri et al. carried out a 3D numerical study on the aerodynamic performance of a centrifugal compressor with a high compression ratio, including the impeller eye, impeller, and vanned diffuser [15].

All centrifugal compressor designers want to achieve the highest efficiency as well as a wide operating range. To reach this goal, the inlet guide vane (IGV) is a convenient and economic option for various applications (Fig. 1) [16]. Variable inlet guide vanes are used to generate inlet swirl in the flow upstream of impellers to reestablish optimum impeller incidence for variable mass flow rate at the constant rotational speed [17].

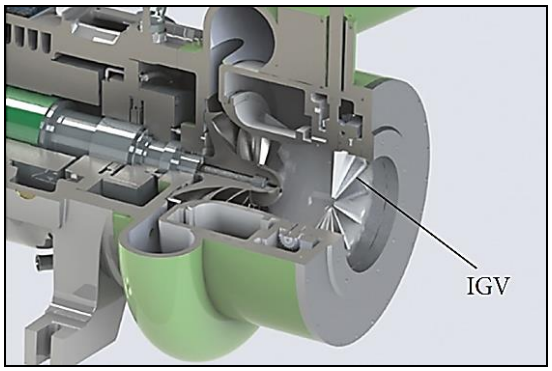

Fig. 1: IGV in centrifugal compressor [18]

IGVs for centrifugal compressors have been thoroughly studied both experimentally and numerically [16, 17, 18, 19, 20].

Since the centrifugal compressor performance is strictly linked to the inlet gas conditions, the design of the inlet of impeller requires careful consideration. In this paper, (a) the theoretical analysis was carried out for optimum designing of the leading edge of centrifugal compressor blades, and, (b) the effect of change in gas conditions on the optimal design of impeller blades leading edge considering the inlet pre-whirl is studied. Hence, considering the ideal gases, three different heat capacity ratio (γ) was applied and their effect of them on the optimum design of the impeller eye was studied. In order to avoid choking, the relative Mach number was limited to 0.9.

2. Limitations of relative velocity at the centrifugal compressor inlet

The inlet eye is a critical region in compressors and requires careful consideration at the design stage. In high-speed centrifugal compressors, it is necessary to limit the maximum relative Mach number (Eq. (1)) at the inlet region to avoid choking and obtain optimum inlet flow conditions. Thus, suitable design of the leading edge of the impeller blades is a crucial factor in centrifugal compressor design.

$$M_r = w/a \tag{1}$$

Since the greatest radius at the inlet is in the shroud region, the maximum relative velocity will occur at the shroud region of the impeller. As presented in reference [21], the mass flow function can be expressed as a function of relative Mach number (M_{rs1}), inlet flow angle (β_{s1}), heat capacity ratio (γ), and the inlet guide vane angle (α_{s1}) (Eq. (2)).

$$f_{s1} = \frac{\dot{m}\omega^2}{\pi k \rho_{01} a_{01}^3} = \frac{M_{rs1}^2 \cos^2\beta_{s1} (\tan\beta_{s1} + \tan\alpha_{s1})^2}{\left[1 + \frac{\gamma-1}{2} M_{rs1}^2 \cos^2\beta_{s1}/\cos^2\alpha_{s1}\right]^{\frac{1}{\gamma-1}+\frac{3}{2}}} \tag{2}$$

For validation, the right-hand side of Eq. (2) is plotted with $\alpha = 30°$ and $\gamma = 1.4$ for different relative Mach numbers in Fig. 2. The results were in complete agreement with the reference [21]. It is obvious that with the enhancement of the relative Mach number, the maximum mass flow will increase. With the limitation considered for inlet flow ($M_{1,rel} = 0.9$), the maximum mass flow will occur at $\beta_{s1} = 49°$, which is the optimum relative angle at the shroud.

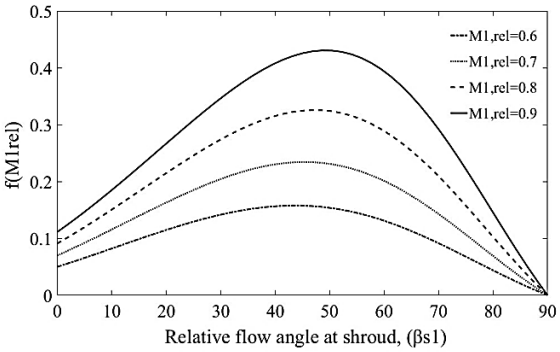

Fig. 2: Mass flow function versus relative flow angle at different relative Mach numbers ($\alpha = 30^{\circ}$, and $\gamma = 1.4$), (in full accordance with reference [21])

3. Optimum angle for the leading edge of Impeller blades

To achieve the optimum design for the leading edge of blades, it is necessary to consider the optimum angle for the shroud region. Conducting analysis for an arbitrary radius ($r_n = nr_{s1}$; $0 < n < 1$), as indicated in Fig. 3 and from the velocity triangle, it can be written as (Eq. (3) and Eq. (4)):

$$C_{x1} = C_{xn} = W_n \cos\beta_n \tag{3}$$

$$U_n = \omega r_n = \omega n r_{s1} = n U_{s1} = w_n \sin\beta_n + c_n \sin\alpha_n = w_n \cos\beta_n (\tan\beta_n + \tan\alpha_n) \tag{4}$$

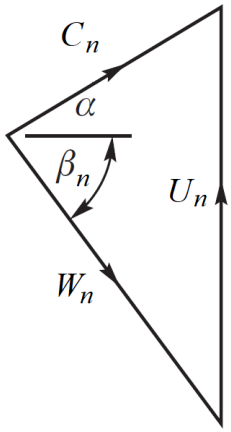

(a)

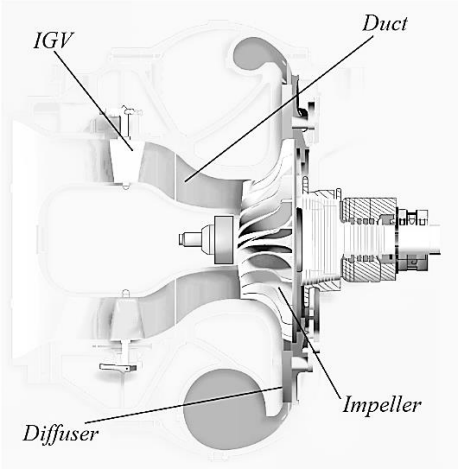

(b)

Fig. 3: a) Velocity triangle at inlet considering the pre-whirl. b) meridional view of a centrifugal compressor

By definition of $k = 1 - (r_{h1}/r_{s1})^2$, and applying the equation of continuity (Eq. (5)),

$$\frac{\dot{m}n^2\omega^2}{\rho_1 k\pi} = W_n^2 \cos^2\beta_n (\tan\beta_n + \tan\alpha_n) \tag{5}$$

The absolute and relative Mach number are related as follows (Eq. (6)),

$$M_1 = C_{x1}/a_1 = M_{rn}\cos\beta_n = M_{rs1}\cos\beta_{s1} \tag{6}$$

Eventually, using the relations of perfect gases, Eq. (5) is written as Eq. (7).

$$\frac{\dot{m}n^2\omega^2}{\pi k\gamma p_{t1}(\gamma RT_{t1})^{1/2}} = \frac{M_{rn}^3 \cos^3\beta_n (\tan\beta_n + \tan\alpha)^2}{\left[1 + \frac{\gamma-1}{2} M_{rn}^2 \cos^2\beta_n / \cos^2\alpha\right]^{\frac{1}{\gamma-1}+\frac{3}{2}}} \tag{7}$$

For a perfect gas, $a_{t1} = \sqrt{(\gamma RT_{t1})}$, and $a_{t1}/a_1 = [1 - (\gamma - 1)(M_1^2)/2]^{1/2}$, thus Eq. (7) is reworked to give Eq. 8:

$$f(M_{rn}, \beta_n, \alpha, \gamma) = \frac{\dot{m}n^2\omega^2}{\pi k \rho_{t1} a_{t1}^3} = \frac{M_n^3 \cos^3\beta_n (\tan\beta_n + \tan\alpha)^2}{\left[1 + \frac{\gamma-1}{2} M_n^2 \cos^2\beta_n / \cos^2\alpha\right]^{\frac{1}{\gamma-1}+\frac{3}{2}}} \tag{8}$$

Equation 8 demonstrates the mass flow function, based on the analysis done for an arbitrary radius, r_n. With the Comparison of Eq. (2) and (8), Eq. (9) can be acquired.

$$f(M_{rn}, \beta_n, \alpha_n, \gamma) = n^2 \times f_{s1} \quad ; \quad 0 < n < 1 \tag{9}$$

As mentioned before, to have an optimum design for the leading edge of impeller blades, the relative Mach number should be limited. Since the maximum relative velocity takes place near the shroud, this region should be considered the critical one. Indeed, other points of the leading edge must be designed based on the optimum

design of shroud radius. Therefore, it is wise to apply for the critical relative Mach number ($M_r = 0.9$) for the shroud radius (r_{s1}) and relate the mass flow function (Eq. (8)) to the relative Mach number at the shroud.

Since $\alpha = cte.$, thus, $C_1 = C_n$. By the definition of absolute Mach number and based on the velocity triangle at the inlet region of blades,

$$M_n = \frac{C_n}{a_1} = \frac{C_1}{a_1} = \frac{w_n(\cos\beta_n/\cos\alpha)}{a_1} = \frac{w_1(\cos\beta_{s1}/\cos\alpha)}{a_1} \Rightarrow \quad (10)$$

$$M_{rn}(\cos\beta_n) = M_{rs1}(\cos\beta_{s1})$$

Substituting $M_{rs1} = 0.9$ and $\beta_{s1} = \beta_{opt,s}$ in to Eq. (10), we get,

$$M_{rn} = \frac{0.9\times(\cos\beta_{opt,s})}{\cos\beta_n}$$

Thus, the mass flow function becomes,

$$f(\beta_n,\alpha,\gamma) = \frac{\left(0.9\times(\cos\beta_{opt,s})\right)^4\times(\tan\beta_n+\tan\alpha)^2}{\left[1+\frac{\gamma-1}{2}\left(0.9\times(\cos\beta_{opt,s})\right)^2/\cos^2\alpha\right]^{\frac{\gamma}{\gamma-1}+\frac{3}{2}}} \quad (11)$$

Eq. (11) looks rather cumbersome and complicated. But indeed, this equation is quite useful. The effect of pre-whirl on the mass flow function can be determined by specifying the value of α. Also, the effect of specific heat capacity ratio (γ) on the mass flow function can be evaluated. Eventually, choosing a particular value for relative Mach number at shroud as a limit ($M_{rs} = 0.9$, in this study) the optimum values for relative angles at different radii (r_n), for maximum mass flow, can then be calculated.

4. Results and discussion

As was mentioned, the inlet configuration and inlet flow structure are known significantly to affect the centrifugal compressor performance. Centrifugal compressors are required to increase their operating range and efficiency, which are limited at low mass flow rates by the rotating stall and surge [22, 23]. In order to suppress the tendency to critical working conditions and extend the operating range at low flow rates, inlet swirl is often considered through the application of inlet guide vanes [21]. Limiting the relative Mach number to 0.9 at the inlet region to avoid choking, and considering γ =1.4, the right-hand side of Eq. (11) is plotted at different pre-whirl in Fig. 4. It can be seen that with growth in pre-whirl angle (α), the maximum mass flow function increases at first and then declines. Conversely, the optimum blade angle (β) decreases at first and then increases. Fig. 5 (a) shows that the maximum mass flow will occur at a pre-whirl angle of 58.75°. Considering the mass flow function as an objective function, the sensitivity analysis for the optimum angle of IGV is shown in Fig. 5(b). As shown, the angle of IGV is sensitive to mass flow function

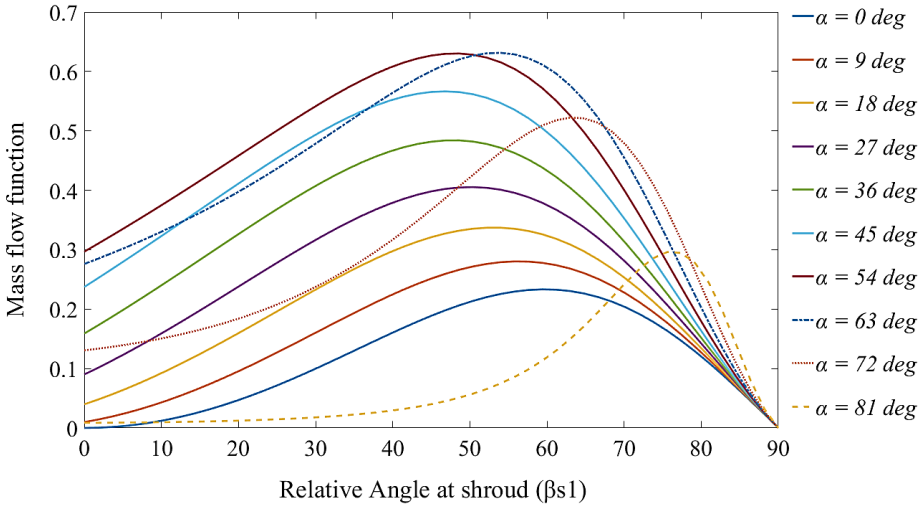

Fig. 4: Change in Mass flow function versus relative angle at shroud for different angle of IGV

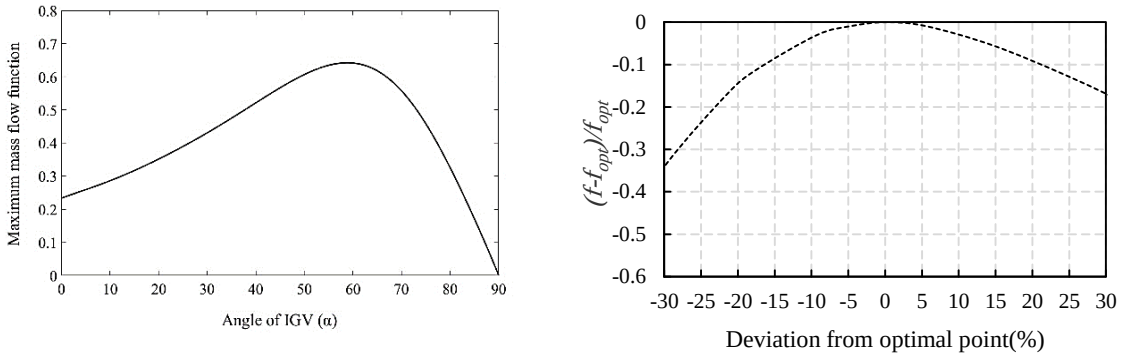

(a) (b)

Fig. 5: (a)Maximum mass flow function versus angle of IGV, and (b) Sensitivity analysis for IGV angle

Examination of the specific heat capacity ratio of different gases at different temperature conditions revealed that the values are approximately in the range of 1.13 to 1.67 [24]. Therefore, the smallest and largest values with an intermediate value are considered to study the effect of specific heat capacity ratio on the optimal design of impeller blades' leading edge. Hence, three different specific heat capacity ratios (γ = 1.13, 1.4, 1.67) were applied. Gases were considered ideal and the relative Mach number was limited to 0.9. The contour plot in Fig. 6 illustrates the variation of mass flow function in terms of relative flow angle (ß) and angle of IGV (α) for different specific heat capacity ratios. Results showed that the maximum achievable mass flow function for γ = 1.13, was about 0.77 and occurred at $\alpha = 60.3°$, $\beta = 48.2°$. For γ = 1.4, the maximum achievable mass flow function was about 0.64 and occurred at $\alpha = 59°, \beta = 51°$. For the case of γ = 1.67, the maximum mass flow function was obtained at about 0.55 and took place at $\alpha = 57.9°, \beta = 52.7°$.

a) γ = 1.13
b) γ = 1.4
c) γ = 1.67

It is obvious that with the growth in heat capacity ratio, the maximum achievable mass flow function was reduced.

Applying Eq. (9), the right-hand side of Eq. (11) is plotted in Fig. 7 with α = 15°, 30°, 45°, and 60°, for different specific heat capacity ratios. As mentioned, the maximum relative velocity takes place near the shroud. Thus, by specifying the optimum angle of the blade in the shroud radius (the maximum value of the Eq. (2) at $M_r = 0.9$), the optimum blade angle at different radiuses can be obtained from Fig. 7.

a) α = 15° b) α = 30°
c) α = 45° d) α = 60°

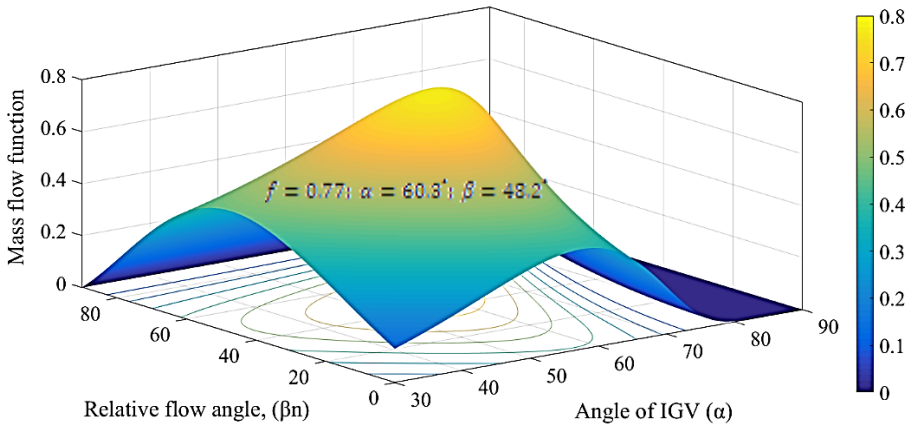

a) γ = 1.13

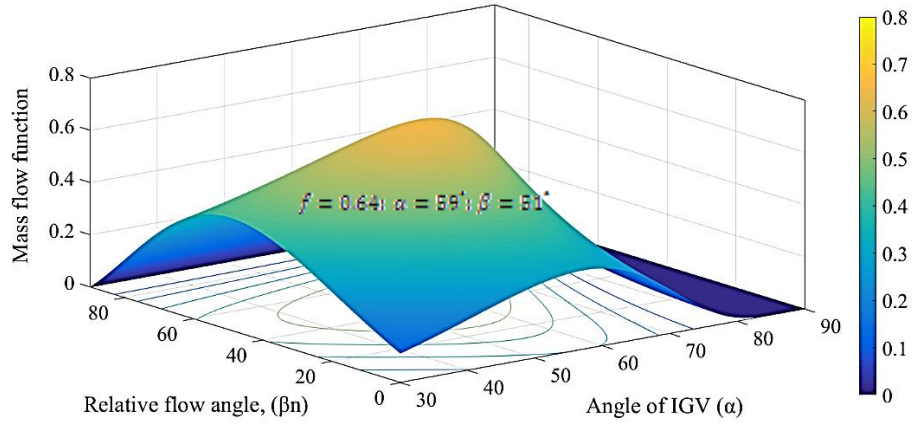

b) γ = 1.4

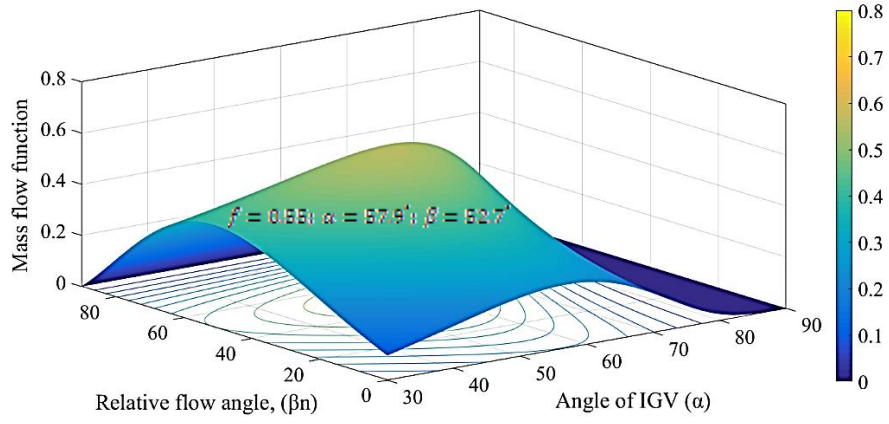

c) γ = 1.67

Fig. 6: Maximum mass flow function in terms of relative flow angle and angle of IGV for different specific heat capacity ratio

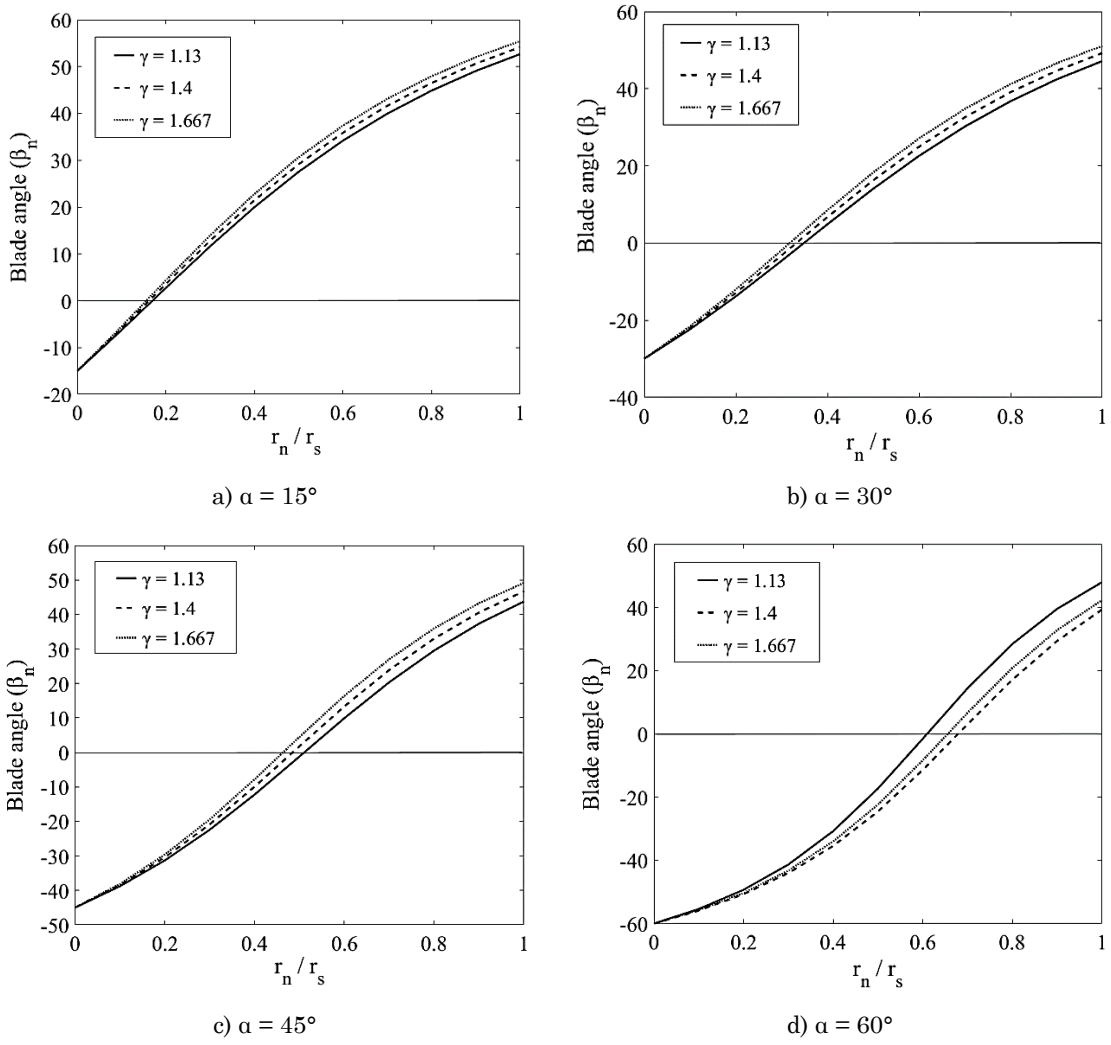

Fig. 7: Optimum blade angle at leading edge of Impeller for different pre-whirl angle

Results showed that with growth in specific heat capacity ratio, the optimum blade angle was increased. But, the changes are not significant. Indeed, the difference was less than 8 percent. A remarkable point in Fig. 7, is the presence of a negative blade angle at low radiuses, which leads to a bad design for an impeller. Considering this limitation will specify the hub radius, in the optimum design of the inlet region of the impeller. Considering the case of α = 30° (which is usual for pre-whirl); as can be seen in Fig. 7 (b), the hub to shroud radius should not be less than 0.33 for a specific heat capacity ratio of 1.4. This limitation is about 0.35 for γ = 1.13 and 0.32 for γ = 1.667. It is obvious from Fig. 7 (a, b, c, d) that the interval between hub to shroud radius will reduce by increasing the pre-whirl angle (α).

5. Conclusions

In this paper, a theoretical investigation was applied to study the effect of change in gas conditions on the optimal design of centrifugal compressor impeller blades leading edge in the presence of IGV. Thus, considering the ideal gases, three different heat capacity ratios (γ = 1.13, 1.4, 1.67) were applied. Knowing that the maximum relative velocity will occur at the shroud region, the relative Mach number was limited to 0.9 to avoid choking.

Results showed that with growth in pre-whirl angle (α), the maximum mass flow function increased at first and then declined. Conversely, the optimum blade angle (β) decreased at first and then increased. The maximum mass flow occurred at a pre-whirl angle of 59° for γ = 1.4. With the growth in heat capacity ratio, the maximum achievable mass flow function was reduced. Results showed that with growth in specific heat capacity ratio, the optimum blade angle was increased. But, the changes were not significant.

The maximum achievable mass flow function for γ = 1.13, was about 0.77 and occurred at α=60.3°, β=48.2°. For γ = 1.4, the maximum achievable mass flow function was about 0.64 and occurred at α=59°, β=51°. For the case of γ = 1.67, the maximum mass flow function was obtained at about 0.55 and took place at α=57.9°, β=52.7°.

It was found that there is a limitation for the hub to shroud radius ratio in impeller design. For the case of α = 30°, the hub to shroud radius should not be less than 0.33 for a specific heat capacity ratio of 1.4. This limitation was about 0.35 for γ = 1.13 and 0.32 for γ = 1.667. The interval between hub to shroud radius is reduced by increasing the pre-whirl angle.

Nomenclatures

a	*Speed of sound (ms^{-1})*
a_t	*Stagnation speed of sound (ms^{-1})*
C	*Absolute velocity of flow (ms^{-1})*
C_x	*Normal component of absolute velocity (ms^{-1})*
f	*Mass flow function*
f_s	*Mass flow function at shroud*
k	*Dimensionless parameter $(1-(r_{h1}/r_{s1})^2)$*
M_r	*Relative Mach number*
M_{rs1}	*Inlet relative Mach number at shroud*
M_{rn}	*Relative Mach number at arbitrary radius*
M_n	*Mach number at arbitrary radius*
$\dot{m}$	*Mass flow rate ($kg\ s^{-1}$)*
n	*Variable between 0 to 1*
r_{s1}	*Shroud radius at inlet (m)*
r_{n1}	*Arbitrary radius at inlet (m)*
U	*Tangential speed (ms^{-1})*
W	*Relative velocity (ms^{-1})*

Greek Symbols

α	*Absolute angle of Inlet Guide Vanes (°)*
β_n	*Relative blade angle at radius r_n (°)*
$\beta_{opt,\ s}$	*Optimum blade angle at shroud (°)*
β_{s1}	*Relative blade angle at shroud (°)*
ρ_t	*Total Density (kgm^{-3})*
γ	*Specific heat capacity ratio*
ω	*Rotational speed ($rad\ s^{-1}$)*

Compliance with Ethical Standards:

Funding: *There is no funding*

Conflict of Interest: *The author declares that there is no conflict of interest regarding the publication of this paper.*

References

de Campos, G. B., Tomita, J. T., & Bringhenti, C. (2018). Simulation of a centrifugal compressor to obtain the characteristic map through computational effort. *Journal of the Brazilian Society of Mechanical Sciences and Engineering*, *40*(2), 1-12.

Krain, H. (2005). Review of centrifugal compressor's application and development. *J. Turbomach.*, *127*(1), 25-34.

Han, F., Mao, Y., Tan, J., Zhao, C., & Zhang, Y. (2015). Flow measurement and simulation of a radial inlet for centrifugal compressor. *Proceedings of the Institution of Mechanical Engineers, Part A: Journal of Power and Energy*, *229*(4), 367-380.

Han, F., Mao, Y., & Tan, J. (2016). Influences of flow loss and inlet distortions from radial inlets on the performances of centrifugal compressor stages. *Journal of Mechanical Science and Technology*, *30*(10), 4591-4599.

Song, K., Zhao, B., Sun, H., & Yi, W. (2019). A physics-based zero-dimensional model for the mass flow rate of a turbocharger compressor with uniform/distorted inlet condition. *International Journal of Engine Research*, *20*(6), 624-639.

Park, C. Y., Choi, Y. S., Lee, K. Y., & Yoon, J. Y. (2012). Numerical study on the range enhancement of a centrifugal compressor with a ring groove system. *Journal of mechanical science and technology*, *26*(5), 1371-1378.

Vanyashov, A. D., Karabanova, V. V., & Vasenko, E. M. (2016). Influence analysis of flow entry conditions on the centrifugal compressor impeller blades to integral gasodynamic characteristics in a combine regulation method. *Procedia Engineering*, *152*, 389-394.

Yang, M., Martinez-Botas, R., Zhang, Y., & Zheng, X. (2016). Effect of self-recirculation-casing treatment on high pressure ratio centrifugal compressor. *Journal of Propulsion and Power*, *32*(3), 602-610.

Torregrosa, A. J., Broatch, A., Margot, X., García-Tíscar, J., Narvekar, Y., & Cheung, R. (2017). Local flow measurements in a turbocharger compressor inlet. *Experimental Thermal and Fluid Science*, *88*, 542-553.

Galindo, J., Gil, A., Navarro, R., & Tarí, D. (2019). Analysis of the impact of the geometry on the performance of an automotive centrifugal compressor using CFD simulations. *Applied Thermal Engineering*, *148*, 1324-1333.

Galindo, J., Serrano, J. R., Margot, X., Tiseira, A., Schorn, N., & Kindl, H. (2007). Potential of flow pre-whirl at the compressor inlet of automotive engine turbochargers to enlarge surge margin and overcome packaging limitations. *International journal of heat and fluid flow*, *28*(3), 374-387.

Kim, Y., Engeda, A., Aungier, R., & Amineni, N. (2002). A centrifugal compressor stage with wide flow range vaned diffusers and different inlet configurations. *Proceedings of the Institution of Mechanical Engineers, Part A: Journal of Power and Energy*, *216*(4), 307-320.

Zhang, M., & Zheng, X. (2018). Criteria for the matching of inlet and outlet distortions in centrifugal compressors. *Applied Thermal Engineering*, *131*, 933-946.

Harley, P., Spence, S., Filsinger, D., Dietrich, M., & Early, J. (2015). Meanline modeling of inlet recirculation in automotive turbocharger centrifugal compressors. *Journal of Turbomachinery*, *137*(1).

Zamiri, A., Lee, B. J., & Chung, J. T. (2017). Numerical evaluation of transient flow characteristics in a transonic centrifugal compressor with vaned diffuser. *Aerospace Science and Technology*, *70*, 244-256.

Ma, C., & Li, W. (2019). The influence of low-solidity and slotting combined treatment

method of diffuser vanes on performance of centrifugal compressor. *Journal of the Brazilian Society of Mechanical Sciences and Engineering*, *41*(2), 1-12.

Leufvén, O., & Eriksson, L. (2016). Measurement, analysis and modeling of centrifugal compressor flow for low pressure ratios. *International Journal of Engine Research*, *17*(2), 153-168.

Sun, Q., Ji, C., Fang, J., Li, C., & Zhang, X. (2017). Optimization design of IGV profile in centrifugal compressor. *Mathematical Problems in Engineering*, *2017*.

Mohseni, A., Goldhahn, E., Van den Braembussche, R. A., & Seume, J. R. (2012). Novel IGV designs for centrifugal compressors and their interaction with the impeller. *Journal of Turbomachinery*, *134*(2).

Ji, C. J., Fan, Z. Y., Zhang, Y., & Ji, W. H. (2013). Study on blade profiles of variable inlet guide vanes of centrifugal compressor. *Journal of Thermal Science and Technology*, *12*(2), 131-134.

Whitfield, A., & Abdullah, A. H. (1997, June). The performance of a centrifugal compressor with high inlet Prewhirl. In *Turbo Expo: Power for Land, Sea, and Air* (Vol. 78682, p. V001T03A033). American Society of Mechanical Engineers.

Khalfallah, S., Ghenaiet, A., Benini, E., & Bedon, G. (2015). Surrogate-based shape optimization of stall margin and efficiency of a centrifugal compressor. *Journal of Propulsion and Power*, *31*(6), 1607-1620.

Wu, X., Liu, Y., Liu, R., & Zhao, L. (2016). Surge detection methods using empirical mode decomposition and continuous wavelet transform for a centrifugal compressor *Journal of Mechanical Science and Technology*, *30*(4), 1533-1536.

White, Frank M. (1998). *Fluid Mechanics* (4th ed.). New York: McGraw Hill. ISBN 978-0-07-228192-7.